Proceedings of Ninth World Conference on Earthquake Engineering
August 2-9, 1988, Tokyo-Kyoto, JAPAN (Vol.VI)

9-2-3

SEISMIC PERFORMANCE OF REINFORCED MASONRY SHEAR WALLS

P. B. SHING, E. KLAMERUS, H. SPAEH, and J. L. NOLAND

Department of Civil, Environmental, and Architectural Engineering,
University of Colorado, Boulder, Colorado, U.S.A.

SUMMARY

Sixteen reinforced masonry wall panels have been tested to examine the influence of the amount of reinforcement and applied axial stress on the in-plane cyclic load resistance of masonry shear walls. The experimental results have indicated that brittle shear behavior can be avoided by using an adequate amount of horizontal reinforcement, and that the amount of vertical and horizontal reinforcement has a significant influence on the postcracked ductility and energy-dissipation capability of a wall panel dominated by the shear mode. Moreover, finite element analyses have been conducted to yield good results. However, deficiencies of the smeared crack approach have also been identified.

INTRODUCTION

Reinforced masonry construction can be frequently found in regions of high seismic risk. Depending on the aspect ratio, load condition, and the amount of reinforcement, two distinct failure mechanisms can be identified with masonry shear walls. One is the flexural mechanism that is characterized by the tensile yielding of vertical reinforcement and/or compressive crushing of masonry at critical wall sections. The other is the shear mechanism that is characterized by diagonal tensile cracking. Past experimental studies (Refs. 1-6) have indicated that wall panels that fail in a predominantly shear mode exhibit a more brittle behavior than those dominated by flexural yielding. However, due to the complexity of the shear cracking mechanism, neither effective analytical methods nor rational design criteria have yet been developed to predict and prohibit brittle shear behavior.

To address the above problems, reinforced masonry wall panels have been tested at the University of Colorado, as part of the U.S.-Japan Coordinated Program for Masonry Building Research. The main objective of this study is to investigate the effects of the amount of vertical and horizontal reinforcement, and the applied axial stress on the inelastic cyclic behavior of masonry shear walls. In this paper, the experimental results obtained from sixteen concrete masonry specimens are presented, and the validity of finite element techniques for masonry shear wall analysis is evaluated.

EXPERIMENTAL PROGRAM

Test Specimens As shown in Fig. 1, the specimens were 6-ft. (1.83-m) high and 6-ft. (1.83-m) long, and fabricated with a single wythe of 6x8x16 hollow concrete blocks. They were fully grouted, with uniformly distributed vertical and

horizontal reinforcement. The horizontal reinforcement had 180-degree hooks around the extreme vertical steel. Each specimen had a reinforced concrete top beam and base slab. The vertical reinforcement ran continuously from the base slab to the top beam with 180-degree anchoring hooks. The reinforcement contents of the sixteen specimens are summarized in Table 1. The material properties are listed in Tables 2 and 3.

Test Setup and Procedure The schematic of the test setup is shown in Fig. 2. Three servo-controlled hydraulic actuators were used to exert a constant axial load and control the in-plane lateral displacement of a specimen. The specimens were carefully instrumented with strain gages and displacement transducers to detect the first yield of the vertical steel, as well as the shear and flexural deformation of the masonry panel. All specimens, except Specimen 7, were subjected to a prescribed standard lateral displacement history, which consisted of gradually increased fully reversed displacement cycles.

Test Results Two types of distinct inelastic behavior modes have been observed from the test specimens. Of the sixteen specimens listed in Table 1, Specimens 1, 2, and 12 had their ultimate strengths governed by the flexural yielding of the vertical steel and compressive crushing of masonry at the wall toes, and can thus be classified as *flexural* specimens. On the other hand, the ultimate strengths of Specimens 3, 4, 5, 7, 9, 13, 14, and 16 were governed by diagonal tensile cracking. Hence, these specimens are termed *shear* specimens. In addition, Specimens 10 and 15 exhibited a mixed flexural/shear behavior, which had significant flexural yielding, toe crushing, as well as diagonal cracking. Finally, Specimens 6, 8, and 11, which were not subjected to any axial load, developed substantial base sliding. As a result, neither the flexural nor the shear capacities were fully developed in these three specimens. The critical strengths of the sixteen wall specimens are summarized in Table 4.

The inelastic behavior of the wall specimens is highly sensitive to the applied axial stress and the amount of vertical and horizontal reinforcement present. Specimens with a vertical steel ratio of 0.38% and horizontal steel ratio of 0.24% exhibited a predominantly flexural behavior. As shown by the hysteresis curves of Specimen 12 in Fig. 3(a), flexural behavior is relatively ductile. However, flexural specimens with higher axial stresses had a more rapid load degradation due to the more severe toe crushing, but exhibited a higher unloading stiffness at load reversal points. Specimens 9 and 10 had the same amount of vertical steel as Specimen 12, but had a horizontal steel ratio of 0.14%. Specimen 9, which had a 270-psi (1.86-MPa) axial stress, exhibited a brittle shear behavior, while Specimen 10, which was subjected to a 100-psi (0.689-MPa) axial stress, had a relatively ductile flexural/shear behavior, as shown by the hysteresis curves in Figs. 3(b) and 3(c). It is evident from these curves that the rate of load degradation increases as the shear mode becomes more significant.

Specimens with 0.54% and 0.74% vertical steel exhibited a predominantly shear behavior. The ultimate strength of a shear specimen depends on the tensile strength of masonry, the amount of horizontal reinforcement, the dowel action of the vertical steel, and the aggregate-interlock mechanism, which in turn depends on the applied axial stress and truss action of the vertical steel. The ultimate shear strength tends to increase with the applied axial stress, and the amount of vertical and horizontal reinforcement present. However, the reinforcement content seems to have a more significant influence on the postcracked ductility and energy-dissipation capability than on the ultimate shear strength of a wall specimen. This is evident from the hysteresis curves of Specimens 9 and 13 in Figs. 3(c) and 3(d), respectively. Furthermore, it can be observed from Table 4 that shear specimens with 0.38% and 0.54% vertical steel reached their ultimate strengths almost instantaneously right after the major diagonal cracking, while

those with 0.74% vertical steel sustained a fair amount of additional lateral load. This is probably due to the fact that increasing the vertical steel increases the dowel action as well as the aggregate-interlock effect.

ANALYSIS

Non-linear finite element models have not been as well developed for masonry structures as for reinforced concrete structures. Nevertheless, the behavior of fully grouted masonry is expected to be very similar to that of concrete. Hence, the main objective of the analytical study conducted here is to evaluate the validity of finite-element models developed for reinforced concrete in analyzing the inelastic behavior of reinforced masonry wall panels.

Finite Element Model Numerous constitutive models (Ref. 7) have been proposed to characterize the non-linear stress-strain behavior of concrete. Most of these models are based on plasticity theory by which concrete is assumed to be linearly elastic before yielding and exhibit a plastic behavior with strain hardening after yielding. Concrete will eventually crush or crack depending on whether the ultimate compressive or tensile strength is reached. Under a multiaxial stress state, these criteria can be defined in terms of a yield surface and a failure surface in the principal stress space. When the stress state lies between the yield and failure surfaces, the incremental stress-strain relation is governed by the plastic flow rule. In finite element analysis, a smeared crack approach is often used. In this approach, concrete remains as a continuum after cracking.

As a first study, the computer code ABAQUS (Ref. 8) is used for the wall analyses. The reinforced concrete element in the program is based on the smeared crack approach and the constitutive model developed by Chen and Chen (Ref. 7). In addition to the stress criterion, a strain criterion is also adopted for cracking. Furthermore, the model accounts for the tension stiffening effect by allowing a gradual drop of tensile stress after cracking. The associated flow rule is used for the formulation of the incremental stress-strain relation. The concrete model is calibrated with the uniaxial material properties obtained from masonry prism tests (Table 3). The tensile strength of masonry is assumed to be 5% of the compressive strength. The elastic modulus of masonry is assumed to be 2000 ksi, and the Poisson's ratio is 0.16. The ultimate compressive strain is assumed to be 0.005, which is larger than the actual ultimate strain, to account for the fact that the analytical model does not have a strain softening regime after passing the peak strength. The tensile strengths of the reinforcing steel are based on the values listed in Table 2. Each wall is discretized into nine layers of four-node isoparametric elements along each direction. Only monotonic loading is applied in the analyses.

Analytical Results Since the shear cracking behavior is more difficult to model than the flexural behavior, the first analysis was conducted on Specimen 3, which had a distinct shear behavior. However, in spite of numerous diagonal cracks that had occurred in the model, the ultimate strength was still dominated by the flexural mode with severe toe crushing. Subsequently, it has been found that the smeared crack approach does not allow the free opening of a diagonal crack. Hence, to simulate crack opening, it is necessary to set the elastic modulus of the elements along the wall diagonal to zero after cracking has occurred. In the analyses conducted here, only the elastic modulus of the upper three diagonal elements has been set to zero after cracking. As shown in Fig. 4(a), the resulting monotonic load-displacement curve for Specimen 3 is very close to the envelope of the experimentally obtained hysteresis curves. Excellent correlation has also been obtained with Specimen 12, which was dominated by flexure, as indicated in Fig. 4(b). However, for shear specimens with 0.38% and 0.54% vertical steel, the shear cracking loads appear to be underestimated, while the

ultimate shear strengths have been overestimated. The analytical results thus indicate a flexure dominated behavior for these specimens. This is evidently due to the residual strength of the remaining diagonal elements.

CONCLUSIONS

It has been found that the inelastic behavior and failure mechanisms of masonry wall panels are highly sensitive to the applied axial stress and the amount of reinforcement present. Shear failure dominated by diagonal cracking is undesirable and often results in brittle behavior. However, shear failure can be effectively prevented by an adequate amount of horizontal reinforcement. Furthermore, shear specimens with larger amounts of vertical and horizontal reinforcement exhibited better ductilities and energy-dissipation capabilities. The flexural capacity of fully grouted masonry wall panels can be predicted with reasonable accuracy using finite element models developed for reinforced concrete. However, owing to the inherent limitations of the smeared crack approach, the diagonal crack opening of a wall panel cannot be satisfactorily modeled. Hence, finite element analysis using discrete crack modeling could be a more adequate but costly approach.

ACKNOWLEDGMENTS

The study presented in this paper is financially supported by the National Science Foundation under the Grant Nos. CES-8517024 and CES-8658100. The partial support of the Masonry Institute of America, Brick Institute of America-Region 12, Colorado Concrete Masonry Association, and CH2M Hill is gratefully acknowledged. The materials for the wall specimens are contributed by the Concrete Masonry Association of California and Nevada, and the Colorado masonry industry. However, opinions expressed in this paper are those of the writers, and do not necessarily represent those of NSF and other sponsors.

REFERENCES

1. Hidalgo, P. A., Mayes, R. L., McNiven, H. D., and Clough, R. W. (1978). "Cyclic Loading Tests of Masonry Single Piers, Vol. 1 - Height to Width Ratio of 2," *Report No. UCB/EERC-78/27*, Earthquake Engineering Research Center, University of California, Berkeley.
2. Chen, S. W., Hidalgo, P. A., Mayes, R. L., Clough, R. W., and McNiven, H. D. (1978). "Cyclic Loading Tests of Masonry Single Piers, Vol. 2 - Height to Width Ratio of 1," *Report No. UCB/EERC-78/28*, Earthquake Engineering Research Center, University of California, Berkeley.
3. Hidalgo, P. A., Mayes, R. L., McNiven, H. D., and Clough, R. W. (1979). "Cyclic Loading Tests of Masonry Single Piers, Vol. 3 - Height to Width Ratio of 0.5," *Report No. UCB/EERC-79/12*, Earthquake Engineering Research Center, University of California, Berkeley.
4. Priestley, M. J. N., and Bridgeman, D. O. (1974). "Seismic Resistance of Brick Masonry Walls," *Bull. of the New Zealand National Society for Earthquake Engineering*, Vol. 7, No. 4.
5. Priestley, M. J. N. (1977). "Seismic Resistance of Reinforced Concrete Masonry Shear Walls with High Steel Percentages," *Bull. of the New Zealand National Society for Earthquake Engineering*, Vol. 10, No. 1.
6. Priestley, M. J. N., and Elder, D. (1982). "Cyclic Loading Tests of Slender Concrete Masonry Shear Walls," *Bull. of the New Zealand National Society for Earthquake Engineering*, Vol. 15, No. 1.
7. Chen, W. F., *Plasticity in Reinforced Concrete*, McGraw-Hill, New York, 1981.
8. *ABAQUS*, Hibbitt, Karlsson, and Sorensen, Inc., Version 4.5, July, 1985.

TABLE 1. Concrete Masonry Specimens

Wall Specimens	Vertical Steel	ρ_v (%)	Horizontal Steel	ρ_h (%)	Total ρ (%)	Axial Load (kips)	Axial Stress (psi)
1	5 x #5	0.38	5 x #4	0.24	0.62	80	200
2	5 x #5	0.38	9 x #3	0.24	0.62	108	270
3	5 x #7	0.74	5 x #3	0.14	0.88	108	270
4	5 x #7	0.74	5 x #3	0.14	0.88	0	0
5	5 x #7	0.74	5 x #3	0.14	0.88	40	100
6	5 x #5	0.38	5 x #3	0.14	0.52	0	0
7	5 x #7	0.74	5 x #3	0.14	0.88	40	100
8	5 x #5	0.38	5 x #4	0.24	0.62	0	0
9	5 x #5	0.38	5 x #3	0.14	0.52	108	270
10	5 x #5	0.38	5 x #3	0.14	0.52	40	100
11	5 x #7	0.74	5 x #4	0.24	0.98	0	0
12	5 x #5	0.38	5 x #4	0.24	0.62	40	100
13	5 x #6	0.54	5 x #4	0.24	0.78	108	270
14	5 x #6	0.54	5 x #3	0.14	0.68	108	270
15	5 x #6	0.54	5 x #4	0.24	0.78	40	100
16	5 x #7	0.74	5 x #4	0.24	0.98	108	270

TABLE 2. Tensile Strengths of Steel

Bar No.	Yield Strength (ksi)	Ultimate Strength (ksi)
3	56	81
4	67	107
5	64	103
6	65	107
7	72	103

TABLE 3. Compressive Strengths of Masonry

Wall Specimens	Masonry Units (psi)	Mortar Specimens (psi)	Grout Specimens (psi)	Three-Course Prisms (psi)
1,2	2400	3500	4400	2900
3	2400	4000	4400	3000
4,5,6	2400	3000	3000	2600
7,8,9	2400	3000	4000	3000
10,11,12	2600	2700	2900	3200
13,14,15	2600	3000	3800	3300
16	2600	2400	5900	2500

TABLE 4. Critical Strengths of Wall Specimens

Wall Specimens	Yield Strength (kips)	Diagonal Cracking Strength (kips)	Ultimate Strength (kips)	Final Damage Mode
1	60	+82,-76	+87,-78	Flexure
2	66	+82,-84	+83,-98	Flexure
3	-	-,-80	+100,-105	Shear
4	65	+55,-51	+72,-87	Shear
5	82	+60,-60	+89,-84	Shear
6	30	+52,-45	+52,-47	Flexure/Shear/Slide
7	83	+65,-60	+97,-97	Shear
8	35	-	+50,-47	Flexure/Slide
9	76	+92,-92	+96,-96	Shear
10	46*	+60,-58	+69,-67	Flexure/Shear
11	63*	+57,-55	+89,-95	Shear/Slide
12	46*	+69,-70	+71,-71	Flexure
13	90	+109,-115	+109,-116	Shear
14	85	+98,-105	+98,-112	Shear
15	58*	+67,-80	+82,-94	Flexure/Shear
16	101	+87,-85	+120,-121	shear

* Analytical Predictions

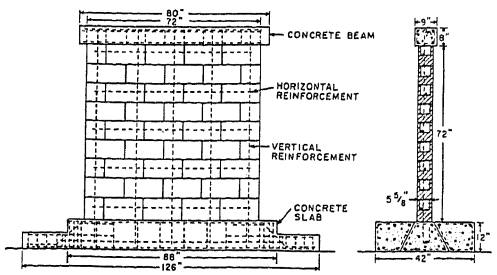

FIG. 1. Test Specimens

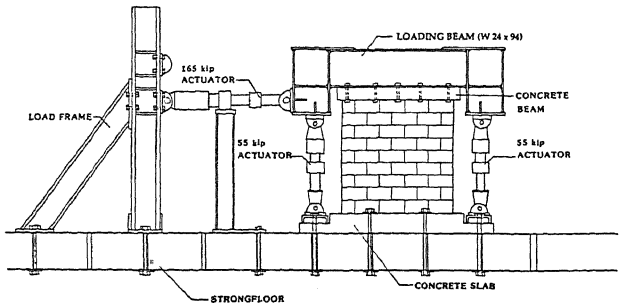

FIG. 2. Test Setup and Apparatus

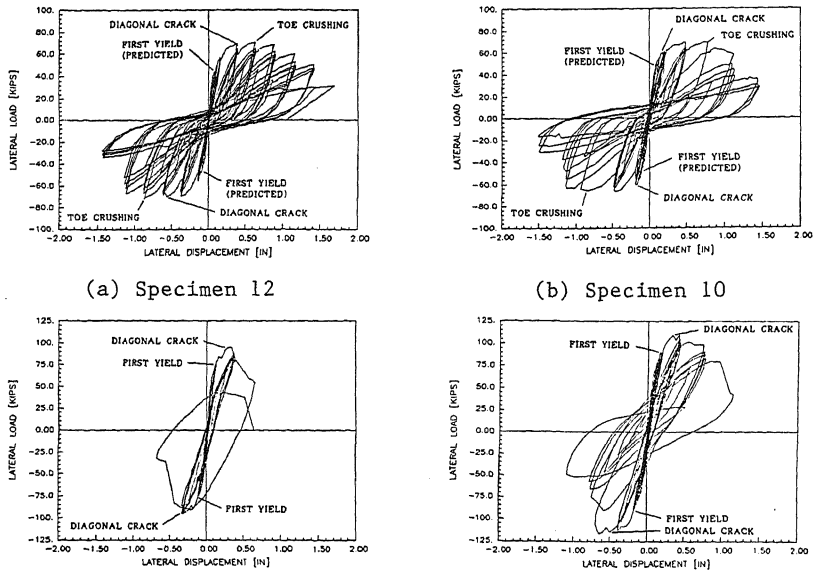

(a) Specimen 12 (b) Specimen 10

(c) Specimen 9 (d) Specimen 13

FIG. 3. Load-Displacement Hysteresis Curves

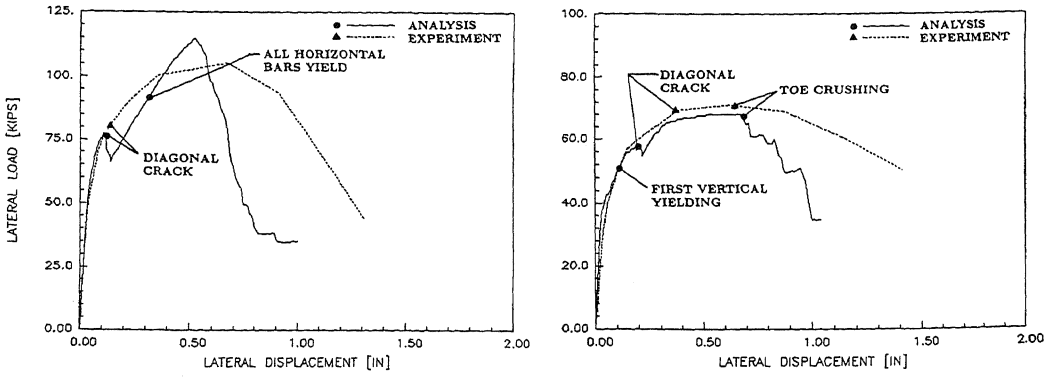

(a) Specimen 3 (b) Specimen 12

FIG. 4. Comparison of Experimental and Analytical Results